WAVELENGTH DEPENDENCE OF THE DUST AEROSOL SINGLE SCATTERING ALBEDO AS OBSERVED BY MRO/CRISM. M. J. Wolff[1] , R. T. Clancy[1], M. D. Smith[2], R. E. Arvidson[3], M. Kahre[4], F. Seelos IV[5], R. V. Morris[6], and The CRISM Science Team, [1]Space Science Institute (18970 Cavendish Rd, Brookfield, WI 53045, mjwolff@spacescience.org), [2]Goddard Space Flight Center (Greenbelt, MD), [3]Washington U. (St. Louis, MO), [4]Ames Research Center (Ames, CA), [5]Applied Physics Laboratory (Laurel, MD), [6]Johnson Space Center (Houston, TX).

Introduction: The fundamental role of dust aerosols in modifying the structure and evolution of the martian atmosphere was first clearly identified by [1]. Through the use of an analytical (simplified) radiative-convective model [2], they demonstrated the inability of a CO_2 atmosphere to reproduce even qualitatively the general thermal structures observed by Mariner 9. More specifically, by including a ``aerosol-like" component that absorbed 10% of the incident solar radiation, one was able to produce temperature profiles in the lower atmosphere that resembled those observed.

[3] carried out a more detailed investigation of the dynamical effects associated atmospheric dust. Through their numerical (1D) radiative-convective model and the Viking observations of aerosol optical depths and atmospheric temperatures, they established that Martian dust possesses the ability to provide both positive and negative radiative feedbacks into dynamical processes.

Not surprisingly, the recognition of the importance of dust in the martian atmosphere naturally led to efforts to characterize the radiative and microphysical nature of the dust particles. Of particular interest is the fraction of incident radiation absorbed, or, more commonly, its complement - the fraction of light scattered, *a.k.a.* the single scattering albedo (*w*). Pollack and collaborators have explored this property in the so-called "solar-band" (0.3-3.0 μm) in a series of papers culminating with that of [4]. Their work is based primarily upon that from Viking and ISM/Phobos and provides a solar band integrated value for *w* of 0.86-0.88. Subsequent work using the MGS/TES solar band channel by [5] finds *w* in the range 0.93-0.94. While these numbers may not appear to be grossly different, they represent a factor two range in implied heating rates! Fortunately, there are currently two visible-near infrared (VIS-NIR) spectrometers currently operating in orbit around Mars that can be used to investigate further this important dust radiative property.

Data: Although both the Mars Express/OMEGA and the Mars Reconnaissance Orbiter/CRISM instruments offer an opportunity to study dust properties in the VIS-NIR, we focus on the CRISM dataset because of the large number and spatial/temporal distribution of "Emission Phase Function" (EPF) sequences available (more 10000 EPFs as of July 12, 2008).

Briefly, an EPF is obtained as part of each "targeted" observation, as well as during "atmospheric-specific" sequences [6]. These will be accomplished through the use of multiple (typically 11) superimposed scans that sweep the slit field-of-view across a target point on the Martian surface as is illustrated in Figure 1. In all cases, hyperspectral data (545 wavelengths) are taken during each of the superimposed images, regardless of the spatial summing used.

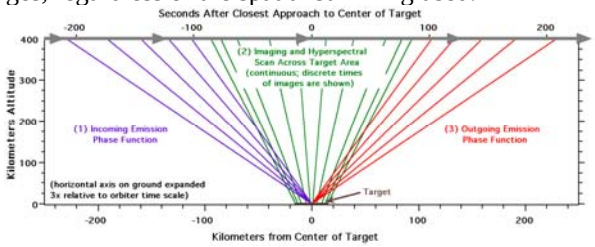

Figure 1 – Schematic of a CRISM EPF sequence illustrating the approach overlapping or "superimposed" images. See [6] for more detail.

Given the generally ill-conditioned nature of aerosol retrieval problems, the ability to retrieve a parameter like the single scattering albedo is greatly enhanced by one's ability to prescribe as many of the needed atmospheric/surface parameters as possible. While atmospheric ground-truth is hard to obtain in Mars remote sensing, the presence of the two MER packages offers a useful approximation, providing both surface reflectance characteristics and total visible optical depth. Additionally, by choosing a very dusty time, one can emphasize the atmospheric effects while minimizing the need for detailed knowledge of surface reflectance characteristics. As a result, we construct a subset of the EPFs that were obtained within a few of both MER sites during the large scale dust event of the 2007 perihelion season (i.e., MY 28) when the Pancam optical depths were > 3. Our dataset consists of 8 EPFs near/at Spirit, 10 near/at Opportunity.

Analysis: Our general approach combines a DISORT-based radiative transfer analysis with non-linear least squares minimization algorithm (MPFIT); see [7] for description and additional references. The general approach is iterative and we outline it very schematically (and briefly) here:

- Initial guess of particle shape: an oblate cylinder (D/L ~ 1) which is a "reasonable" approximation to the Tomasko et al. [8] phase function over the scattering angles primarily sampled by the CRISM EPFs (see Figure 2).

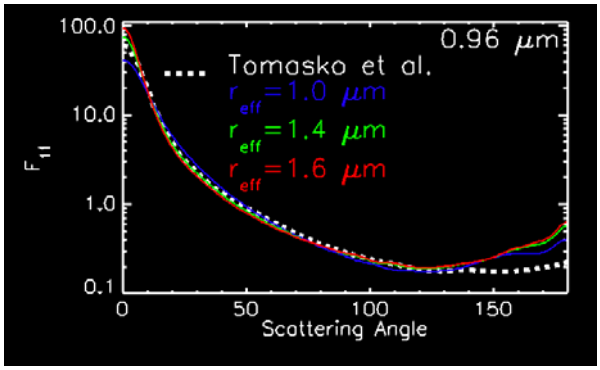

Figure 2 – Representative phase function used in CRISM analyses compared to that of [9]. The scattering angle range (of first scattering) sampled by EPFs near MER sites is typically 90-140 degrees. The "flatness" of the [9] phase function is also seen in terrestrial aerosols, indicating that the idealized shape assumption could clearly be improved.

- Initial guess of the indices of refraction: use that presented in [9] which based in part on the results of [8].
- Initial guess of "Hapke parameters" from MER analyses of [10,11].
- Compute Scattering Properties for a mesh of particle size distributions and current values for refractive indices: Using the T-Matrix codes of Mishchenko and collaborators [12], one computes the forward scattering parameters and phase function for each CRISM channel of interest.

1. Fix optical depth at 0.88 μm using Pancam observations [i.e., 13] and specify surface properties using current values for Hapke parameters.
2. Derive best-fit *w* for each EPF observation.
3. For each retrieved *w*, find associated imaginary part (*k*) of the refractive indices using lookup tables (using a grid of *k* and particle sizes).
4. Find real part of the refractive indices (n) using a Subtractive Kramers-Kronig algorithm (courtesy of K. Snook).
5. Recompute dust scattering properties using new indices and T-Matrix.
6. [Optional] Adjust Hapke "w" parameter using new aerosol properties for a small set of lower dust loading EPF observations. This is more important for the wavelengths beyond the Pancam filter range.
7. Goto 1 if change in $n+ik$ is not "small".

Results: The retrieved single scattering albedo (*w*) values after four iterations are shown in Figure 3 for four of the particle size cases considered. The "error bars" represent the dispersion (or at least the square-root thereof) of the 18 EPF sequences. Note that the assumed particle size is only of consequence for *w* (in our sample) at the shortest and longest wavelengths.

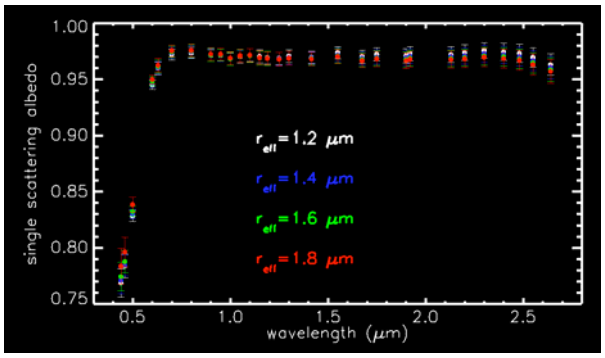

Figure 3 – Resulting *w* values after 4 iterations of the algorithm detailed in the previous section.

A comparison of the CRISM values to previous work, including recent analyses of OMEGA data [e.g., 14, 15] is made in Figure 4. For the NIR range, the agreement between CRISM and OMEGA based results is quite good. Discrepancies in the VIS range appear to be related to the simplified treatment of the scattering phase function (i.e., Henyey-Greenstein, [15]).

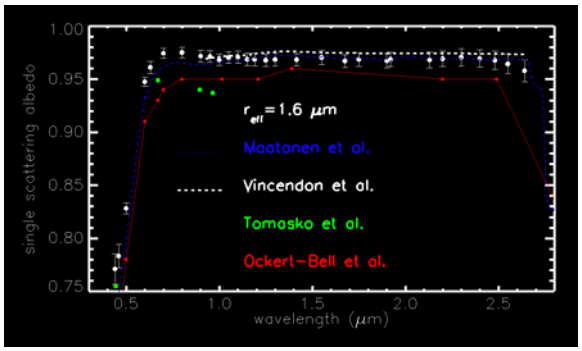

Figure 4 - Comparison of CRISM-based values with previous results. The OMEGA results are consistent with the higher w values found by CRISM in the NIR range. The VIS range discrepancies are likely related to differences in phase function prescriptions.

Parameter uncertainties. Beyond the issue of scattering phase functions, two atmospheric parameters should be considered in terms systematic error sources: uncertainty in Pancam optical depths and in the Hapke "w" reflectance parameter. Figure 5 shows the spread in retrieved single scattering albedo values

as a result of 25% perturbation (red and blue lines) of the adopted Pancam optical depths (white symbols). Although the effects of such a perturbation are non-trivial, they are within the "error bars" of the original retrieved values.

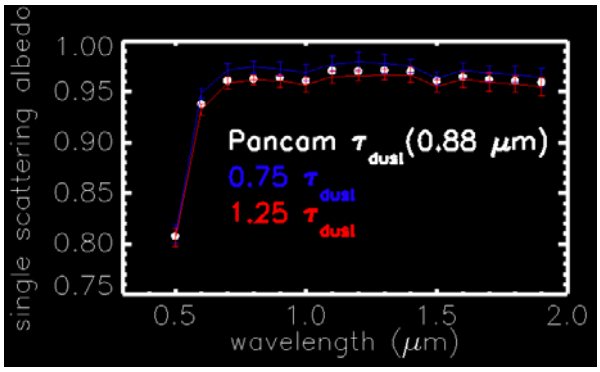

Figure 5 – Spread in single scattering albedo introduced by varying the adopted Pancam optical depth by 25%.

Figure illustrated the impact of a 10% variation on the Hapke "w" parameter. The amplitude of the effect is similar to that of the exercise shown in Figure 5. In both cases, the changes in the retrieved values do not explain the shortwave differences between the CRISM (and OMEGA) values and those of the Viking and Pathfinder analyses.

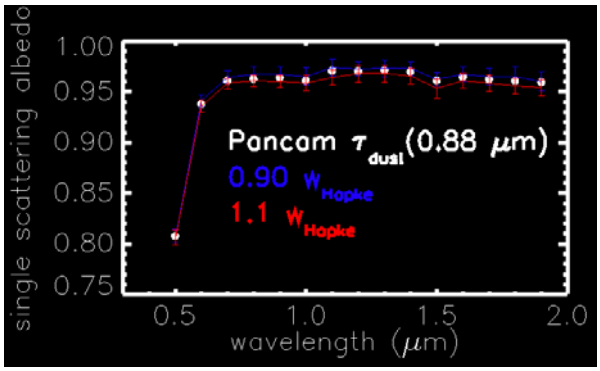

Figure 6 – Spread in single scattering albedo introduced by varying the Hapke "w" parameter by 10%.

Ultimately, the very dusty conditions and the use of "ground truth" via the MER observations/analyses appear to offer a degree of fidelity and robustness that were not available in the previous analyses.

Some Discussion: The single scattering albedo function shown in Figure 3 provides a "solar band" (weighted) albedo of 0.93-0.94, depending upon the assumed particle size distribution. This is quite consistent with the TES-based results reported by [5]; significantly higher than those of [4]. Such values are consistent with OMEGA-based results [15], even without allowing the calibration uncertainties associated with the shortwave detector/channels.

Our approach, though more computationally intense then the use of a simple phase function parameterization (i.e., Henyey-Greenstein), does provide a self-consistent dust aerosol model. Specifically, it provides a set of refractive indices that allow one to compute radiative properties for any desired particle size distribution including the effects of vertical gradients. The *k* function associated with 4 particle size assumptions is shown in Figure 6. Clearly, the utility of such data depends on one's ability to determine the effective size distribution present in the conditions sampled by the 18 EPFs. Fortunately, both numerical modeling and TES limb observations [e.g., 16] indicate that dust loading is the closest to "uniform mixing" during events similar to that of the 2007 perihelion season. Thus, it is imply a question of knowing the particle sizes!

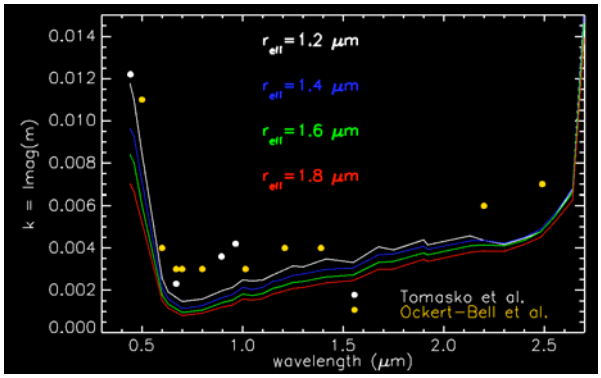

Figure 6 – Imaginary refractive indices derived the CRISM observations under the assumption of 4 specific effective particle sizes.

References: [1] Gierasch, P. J. and Goody, R. M. (1972), *J. Atm. Sci.*, 29, 400. [2] Gierasch, P. J. and Goody, R. M. (1968), *PSS*, 16, 615. [3] Pollack, J. B. et al. (1979), *JGR*, 84, 2929. [4] Ockert-Bell, M. E. et al. 1997), *JGR*, 102, 9039. [5] Clancy, R. T., et al. (2003), *JGR (Planets)*, 108, 5098. [6] Murchie, S. et al. (2007), *JGR*, 112, DOI: 10.1029/2006JE002682. [7] Wolff, M. J. et al. (2006), *JGR Planets*, 111. [8] Tomasko, M. G. et al. (1999), *JGR Planets*, 104, 8987. [9] Wolff, M. J. and Clancy, R. T. (2003), *JGR Planets*, 108, 5097. [10] Seelos, F. P. (2005), Ph. D. Thesis (Washington U.) [11] Johnson J. R. et al. (2006), *JGR Planets*, 111. [12] www.giss.nasa.gov/~crmim/. [13] Lemmon, M. T. et al. (2004)., *Science*, 306, 1753. [14] Vincendon et al. (2007), *JGR Planets*, 112. [15]

Maatanen, A. et al. (2008), submitted to Icarus. [16] Clancy, R. T. et al. (2008), This Meeting.